

---

This manuscript is a preprint and has been submitted for publication in Journal of Sedimentary Research. Please note that, despite having undergone peer-review, the manuscript has yet to be formally accepted for publication. Subsequent versions of this manuscript may have slightly different content. If accepted, the final version of this manuscript will be available via the '*Peer-reviewed Publication DOI*' link on the right-hand side of this webpage. Please feel free to contact any of the authors; we welcome feedback

---

1           **Cenozoic contourites in the eastern Great Australian Bight, offshore southern**  
2           **Australia: implications for the onset of the Leeuwin Current**

3  
4                                   Christopher A-L. Jackson\*

5   Craig Magee

6   Esther R. Hunt-Stewart

7  
8           *Basins Research Group (BRG), Department of Earth Science & Engineering, Imperial*  
9           *College, Prince Consort Road, LONDON, SW7 2BP, UK*

10  
11                                   *\*corresponding author email: c.jackson@imperial.ac.uk*

12  
13   **ABSTRACT**

14  
15   Thermohaline oceanic currents influence global heat transfer, controlling local and global  
16   variations in climate, biodiversity, and the terrestrial biosphere. Paleoceanographic studies  
17   typically use biostratigraphic and geochemical proxies to reconstruct the dynamics of these  
18   currents in Earth's ancient oceans, although seismic reflection data have also been  
19   successfully employed, most commonly in the North Atlantic Ocean. Here we use 2D seismic  
20   reflection data from the Ceduna Sub-basin, Great Australian Bight, offshore southern  
21   Australia to describe middle Eocene-to-Recent contourites deposited within an overall  
22   carbonate-dominated succession. These deposits comprise large (100 m wavelength by up to  
23   50 m tall) bedforms and deep (10–90 m), wide (up to 3 km) erosional scours. The scours are  
24   particularly well-developed at one specific stratigraphic level, defining moats that encircle  
25   Middle Eocene shield volcanoes, which formed syn-depositional bathymetric highs. We  
26   suggest that sediment erosion, transport, and deposition may record middle Eocene initiation  
27   of the Leeuwin Current, one of the most important ocean currents in the southern hemisphere.  
28   Deepest seabed scouring may reflect middle Miocene waxing of the so-called 'proto-Leeuwin  
29   Current', possibly driven by changes in ocean circulation patterns caused by the Miocene  
30   Global Optimum. The results of this seismic reflection-based study are consistent with results  
31   derived from other paleoceanographic proxies, thereby highlighting the continued key role  
32   seismic reflection data have in understanding the occurrence, geographical distribution, and  
33   significance of ancient ocean currents.

34

35 **Introduction.** By influencing seawater temperature and salinity, ocean current activity  
36 controls regional and global trends in climate and biodiversity. Determining past changes in  
37 thermohaline circulation patterns in the world's oceans is thus important to understanding  
38 how climate and biodiversity varied in deep time and, therefore, may change in the future (cf.  
39 “geological analogues” of IPCC, 2007; see also e.g., Henderson, 2002; Wunsch, 2002;  
40 Rahmstorf, 2003; Wyrwoll et al., 2009). Paleoceanographic analysis commonly relies on  
41 biostratigraphic and geochemical proxy data, which: (i) are expensive to collect, and typically  
42 only collected on academic scientific cruises (e.g. IODP); (ii) are spatially limited (i.e.  
43 collected over a relatively small area within a discrete stratigraphic intervals); and (iii) do not  
44 typically provide a physical (i.e. stratigraphic) record of the initiation, extent, and decay of  
45 oceanographic currents (e.g. von Blackenburg, 1999; Henderson, 2002). Seismic reflection  
46 data can image very large (up to 10's of metre thick, and several hundred-to-tens of  
47 kilometres long) contourite systems, which provide an explicit record of ocean current-  
48 driven, erosion and reworking of the ancient seabed (e.g. Boldreel et al., 1998; Davies et al.,  
49 2001; Faugères et al., 1999; Rebesco and Stow, 2001; Stow et al., 2003; Due et al., 2006;  
50 Hohbein et al., 2012; Rebesco et al., 2014). When integrated with more widely used  
51 paleoceanographic proxies, as they have been most commonly and successfully in the North  
52 Atlantic Ocean (e.g. Tucholke, 1979; Tucholke & Mountain, 1979; Mountain & Miller, 1992;  
53 Davies et al., 2001; Müller-Michaelis et al., 2013; Calvin Campbell & Mosher, 2016; Boyle  
54 et al., 2017), seismic reflection data form a key part of the oceanographer's toolkit.

55 In this study we use 2D seismic reflection data from the Ceduna Sub-basin, Great  
56 Australian Bight, offshore southern Australia to identify and map Middle Eocene-to-Recent  
57 contourites, which possibly record the middle Eocene initiation of the current now known as  
58 the Leeuwin Current. Although its age of initiation is debated, the present Leeuwin Current is  
59 the longest (5000 km) and one of the most important ocean currents in the southern  
60 hemisphere (Fig. 1A). It is connected to and samples the global thermohaline system via the  
61 Indonesian Gateway (Feng et al., 2009), flowing southwards at relatively shallow depths  
62 (<300 m) and modest speeds (<2 m s<sup>-1</sup>, but as low as 0.3–0.5 m s<sup>-1</sup> in the Great Australian  
63 Bight) along the western coast of Australia and thereafter eastwards into the Great Australian  
64 Bight (Fig. 1A) (Cresswell and Golding, 1980; Cresswell & Domingues, 2009). Transporting  
65 warm, low-salinity waters derived from the South Equatorial Current within a relatively  
66 narrow band (<100 km), the Leeuwin Current contributes to climatic variations and  
67 vegetation patterns (e.g., Caputi, 2001; Feng et al., 2009; Wyrwoll et al., 2009), and  
68 continent-scale biodiversity patterns by transporting otherwise low-latitude fauna to

69 anomalously high latitudes (e.g., Cann and Clarke, 1993; McGowran et al., 1997; Passlow et  
70 al., 1997). By providing what we think is the first physical evidence for ocean current activity  
71 in relatively deepwater, offshore southern Australia, our seismic reflection-based study  
72 broadly supports studies proposing a middle Eocene initiation age for the Leeuwin Current  
73 (McGowran et al., 1997; see also Feary and James, 1995, 1998). More generically, our study  
74 confirms that seismic reflection data, if integrated with biostratigraphic and geochemical  
75 proxies, can help improve our understanding of deep-time dynamics of the Earth's ancient  
76 oceans.

77

78 **Geological Setting.** The Ceduna Sub-basin is located in the Bight Basin, offshore southern  
79 Australia (Fig. 1A), and formed in response to Jurassic-to-Early Cretaceous rifting and Early  
80 Cretaceous-to-Recent, post-rift thermal subsidence. Numerous submarine volcanoes were  
81 emplaced during earliest Middle Eocene magmatism at *ca.* 42 Ma (the 'Bight Basin Igneous  
82 Complex'; Schofield & Totterdell, 2008; Jackson, 2012; Magee et al., 2013), with the  
83 volcanoes overlapped by the fully marine, Middle Eocene-to-Recent, carbonate-dominated  
84 Nullarbor Limestone (Fig. 1B) (Schofield & Totterdell, 2008). Schofield & Totterdell (2008)  
85 and Jackson (2012) identify numerous 'scours' in the Nullarbor Limestone, although they do  
86 not explore their age or origin, their genetic relationship to the Middle Eocene volcanoes, or  
87 the potential paleoceanographic significance of their causal current. There are no direct  
88 constraints on Middle Eocene-to-Recent water depths in the distal Ceduna Sub-basin,  
89 although the heights of Eocene clinoforms along the northern basin margin (Feary and James,  
90 1995, 1998; McGowran et al., 1997) and the preservation of pristine submarine volcanoes  
91 within fully marine sediments (Magee et al., 2013; Jackson (2012) suggests the basin  
92 deepened to a few hundred metres (i.e. broadly comparable to the present depth of the  
93 Leeuwin Current; see above) during middle Eocene flooding (see also McGowran et al.,  
94 1997; Shafik, 1983; 1990). The Ceduna Sub-basin lies outboard of the modern day shelf edge  
95 in water depths of 200–4000 m; the seabed in the study area is below the influence of the  
96 modern Leeuwin Current, which extends to depths of 300 m (Feng et al., 2009).

97

98 **Paleoceanography of the Great Australian Bight.** The Quaternary extent and dynamics of  
99 the Leeuwin Current in the Great Australian Bight are relatively well understood (Cresswell  
100 and Golding, 1980; Feng et al., 2009; Wyrwoll et al., 2009), whereas its timing of initiation,  
101 and its pre-Quaternary eastward 'reach' into the Great Australian Bight, remain uncertain.  
102 Based on their discovery of warm-water, Eocene microfauna in the Otway Basin, McGowran

103 et al. (1997) suggested an even older, Middle Eocene age of initiation for the Leeuwin  
104 Current in the Great Australian Bight, arguing these fauna were likely derived from warm  
105 low-latitudes (i.e. via the proto-Leeuwin Current) and not cold high-latitudes (i.e. via the  
106 Flinders Current) (Fig. 1A); this interpretation is supported by fully coupled climate model  
107 simulations (Huber et al., 2004). However, pre-Early Oligocene initiation of the Leeuwin  
108 Current is disputed given that opening of the Tasmanian Gateway, which facilitated  
109 eastwards flow of warm ocean waters along southern Australia into the Pacific, did not occur  
110 until the Early Oligocene (e.g. Stickley et al., 2004; Wyrwoll et al., 2009). These studies  
111 together suggest the proto-Leeuwin Current in some way shaped the Eocene-to-Recent  
112 stratigraphic evolution of the Great Australian Bight shelfal regions, although the  
113 stratigraphic expression of time-equivalent, basin-centre units, which should also record the  
114 initiation and influence of this important ocean current, has yet to be documented.

115 Although Middle Eocene initiation of the Leeuwin Current is disputed, there is  
116 evidence from IODP Leg 182 that anomalously warm waters entered the Great Australian  
117 Bight during the middle Miocene, possibly in response changes in ocean circulation driven  
118 by the Miocene Climatic Optimum (e.g. Savin et al., 1975; Feary and James, 1995, 1998;  
119 Gourley and Gallagher, 2004). For example, McGowran et al. (1997) document the ‘Little  
120 Barrier Reef’, a thick (350 m), laterally extensive (>475 km long), rimmed carbonate  
121 platform developed along the northern margin of the Bight Basin (Fig. 1A).

122

123 **Data and methods.** Our dataset consists of 109 time-migrated, zero-phase, 2D seismic  
124 reflection lines that have a cumulative line length of *c.* 13,000 km and cover *c.* 44,000 km<sup>2</sup> of  
125 the central Ceduna Sub-basin (Fig. 1A). The NW- and NE-trending lines are spaced 4–16 km  
126 and 4–8 km, respectively (Fig. 2). The Gnarlyknots-1a borehole constrains the age of four  
127 key seismic reflections (Horizons A–D; Figs 1B and 3). This borehole also contains well-log  
128 data indicating the relatively thin (<300 m) Nullarbor Limestone has a fairly constant P-wave  
129 velocity of 2100 m s<sup>-1</sup> (cf. Espurt et al., 2009); this allows us to convert measurements in  
130 milliseconds two-way time (ms TWT) to metres (e.g. 100 ms TWT=105 m). Extrusive  
131 igneous bodies were identified and mapped using the geometric and geophysical criteria  
132 outlined by Totterdell & Schofield (2008), Jackson (2012) and Magee et al. (2013). Our 2D  
133 seismic lines are widely spaced relative to the size of the intra-Nullarbor features we describe  
134 below, meaning we cannot document their full, three-dimensional external form or internal  
135 architecture (cf. Calvin Campbell & Mosher, 2016). However, intra-Nullarbor scours and  
136 ‘mounded’ seismic facies are typically imaged on and can be mapped between, several

137 adjacent seismic lines. In particular, it is clear that the scours are only developed adjacent to  
138 and define ‘moats’ that encircle the volcanic vents (Figs 2 and 3).

139

140 **Description of intra-Nullarbor seismic facies.** We define two main stratal units within the  
141 Nullarbor Formation (SU1-2), separated by a major erosional surface (Horizon D; Figs 1 and  
142 3). The base of SU1 is defined by a high-amplitude, laterally-continuous, positive seismic  
143 reflection defining the contact between the Pidinga Formation and the Nullarbor Limestone  
144 (i.e. Horizon B), or a series of volcanoes (i.e. Horizon C) (Figs 1B and 3). SU1 comprises the  
145 lower part of the Nullarbor Limestone and, away from the volcanoes, is typically  
146 characterised by low-to-moderate amplitude, parallel-to-sub-parallel, very continuous  
147 reflections (Fig. 3). Closer to the volcanoes (i.e. <2 km), a series of gently-dipping (<4°)  
148 reflections are developed in SU1, and these locally display bilateral downlap onto the  
149 underlying reflections and thus define convex-up, ‘mounded’ bodies (Figs 3B-D). These  
150 inclined reflections, which either dip towards (Fig. 3A) or away (Figs 3C–D) from the  
151 volcanoes, typically overlie low-angle (<6°) erosional surfaces, which are up to 2 km wide  
152 and display up to 100 m of relief; these surfaces pass laterally into (seismically) conformable  
153 surfaces (Fig. 3).

154 The base of SU2 is locally defined by a major erosion surface along which numerous  
155 scours are developed (Horizon D; Figs 1–3). These scours locally define a series of ‘moat-  
156 like’ features that fully or partly encircle 15 of the 57 vents present in the Ceduna Sub-basin  
157 (e.g. Fig. 2). The scours have a relief of 10–90 m, extend <3 km from the volcanoes, and  
158 their flanks dip 0.1–6.1°, being best-developed around volcanoes that are typically >200 m  
159 tall. Some of the scours are asymmetric, consisting of a long, gently dipping outer margin  
160 inclined towards the vents and a shorter, more steeply-dipping surface that dips away from  
161 the vents (Figs 3B–D). However, our 2D seismic data do not allow us to confidently  
162 determine if the scours are consistently asymmetric in one direction, or if they are  
163 preferentially developed on one side of the vents (Fig. 2). Two main types of seismic facies  
164 fill the scours: (i) high-amplitude, ‘mounded’ reflections, which have a relief of up to 50 m  
165 and a distance of 100–200 m between adjacent mound crests (Fig. 3B); and (ii) low-to-high  
166 amplitude, gently-dipping (<2°), moderately discontinuous to laterally-continuous reflections  
167 (Fig. 3). The upper part of SU2 is dominated by low-to-high amplitude, flat-lying to gently-  
168 dipping (<2°), laterally-continuous reflections (Fig. 3), with erosionally based packages of  
169 chaotic reflections being locally developed.

170

171 **Interpretation of intra-Nullarbor features.** Based on their development in a fully marine  
172 succession and given that post-Middle Eocene water depths were probably at least several  
173 hundred metres (see Jackson, 2012), it is unlikely the intra-Nullarbor scours and mounds  
174 formed subaerially. Furthermore, the coeval basin margin, which was likely located several  
175 hundred kilometres to the north, was carbonate-dominated and constructional (Fig. 1; see also  
176 Feary and James, 1995, 1998), suggesting only limited sediment bypass to deep-water, and  
177 that voluminous, strongly erosional gravity currents, such as turbidity currents, were likely  
178 not responsible for the formation of the intra-Nullarbor scours and mounds. Although large  
179 mounded bodies, typically interpreted as sediment waves, are commonly observed in many  
180 deepwater depositional systems, scours of the irregular shape and size to those observed here  
181 are not (e.g. Posamentier & Kolla, 2003).

182         Based on their development in a fully marine succession deposited in several  
183 hundreds of metres of water, our preferred interpretation is that the scours formed in response  
184 to ocean current-related incision of the seabed (Fig. 4). Such scours are common in modern  
185 seas and oceans, typically in association with channel-related contourite drifts (*sensu* Stow et  
186 al., 2002). The spatial restriction of Ceduna Sub-basin scours to within c. 3 km of the  
187 volcanoes, strongly suggests the volcanic edifices formed syn-incision bathymetric highs that  
188 perturbed the velocity structure of the causal ocean currents. We suggest this perturbation  
189 increased current turbulence and, most critically, seabed shear stress, driving localised  
190 erosion of the seabed immediately adjacent to the volcanoes (Fig. 4) (e.g. O'Reilly et al.,  
191 2003; MacLachlan et al., 2008). Submarine scours of broadly similar geometry, dimension,  
192 and origin are observed adjacent to igneous rock-cored bathymetric highs in the Pisces Reef  
193 system, Irish Sea, UK (Callaway et al., 2009), and in the Capel and Faust basins, offshore  
194 eastern Australia (Rollet et al., 2012). Scours are best-developed adjacent to the tallest  
195 volcanoes because only these were expressed at the paleoseabed at the onset of the ocean  
196 current initiation (see below); shorter volcanoes were buried by this time, thus they lack  
197 flanking scours.

198         We interpret that inclined and mounded reflections developed throughout the  
199 Nullarbor Limestone represent dip-oblique and dip-parallel sections, respectively, through  
200 contourite drifts (cf. Rebesco and Stow, 2001; Stow et al., 2003; Hohbein et al., 2012;  
201 Rebesco et al., 2014). Sedimentary bodies like this are commonly associated with seabed  
202 scours, being deposited when bottom current energy is low enough to permit sediment  
203 reworking within bedforms (Fig. 4) (e.g. Stow et al., 2002). Like the scours, intra-Nullarbor  
204 bedforms are spatially restricted to within a few kilometres of the vents, suggesting they too

205 formed due to volcano-driven perturbations in ocean current velocity and seabed shear stress.  
206 In their case, however, an increase in seabed shear stress was only sufficient to rework  
207 sediment and not deeply erode the seabed (Fig. 4).

208

209 **Implications for the paleoceanographic development of the Great Australian Bight.**

210 Although the Gnarlyknots-1a borehole penetrates the Nullarbor Formation, no  
211 biostratigraphic data were collected; as a result, we cannot constrain the age of intra-  
212 Nullarbor scours, associated strata, or indeed, the causal current more tightly than ‘middle  
213 Eocene-to-Recent’. Furthermore, no paleobathymetric data (e.g. benthic foraminifera) were  
214 collected in Gnarlyknots-1a, meaning we have no direct constraints on water depth variations  
215 during the middle Eocene-to-Recent, and thus the depth of formation of the ocean current-  
216 related scours and bedforms remains uncertain (see also discussion in Jackson, 2012). Our  
217 relatively widely spaced 2D seismic reflection data also do not allow us to confidently  
218 determine if intra-Nullarbor scours are preferentially developed on one, most likely the  
219 down-current (i.e. lee) side of the seabed obstruction (i.e. the volcanoes), or if the associated  
220 bedforms are best-developed on one, most likely the up-current side of the vents, and display  
221 down-current accretion (e.g. Callaway et al., 2009; Rollet et al., 2012). Because of this, we do  
222 not know the dominant direction of the causal current.

223 Notwithstanding these limitations, it is informative to discuss the implications of our  
224 study for the Paleogene paleoceanographic evolution of the eastern Great Australian Bight.  
225 Using biostratigraphic proxy data from the Bight and Otway basins, McGowran et al. (1997)  
226 suggest the initiation of eastwards protrusion of a so-called ‘proto-Leeuwin Current’ into the  
227 Great Australian Bight during the middle Eocene, with further evidence for its presence in the  
228 middle Miocene (Fig. 1A; see also Feary and James, 1995, 1998). This interpretation was,  
229 however, challenged by Wyroll et al. (2009), who suggest these fauna may simply record  
230 locally elevated sea surface temperatures unrelated to the initiation of a plate-scale  
231 thermohaline current. We here suggest middle Eocene-to-Recent contourites developed in the  
232 Ceduna Sub-basin are associated with Paleogene initiation of an oceanographic current,  
233 which we link to the postulated proto-Leeuwin Current, and which operated in broadly  
234 similar waters depths (i.e. a few hundred metres) to the present Leeuwin Current (Fig. 4).  
235 More specifically, we propose these features record late middle Eocene initiation and  
236 subsequent fluctuations in the strength and erosivity of, the current. The major intra-  
237 Nullarbor erosion surface (Horizon D), for example, which is best-developed immediately  
238 adjacent to the volcanoes, may represent intensification or ‘waxing’ of the proto-Leeuwin



239 Current (Fig. 4). Despite a lack of age data, we tentatively suggest this erosional event, and  
240 related bedforms, may be the stratigraphic expression of the Miocene Climatic Optimum-  
241 related event proposed by Feary and James (1995, 1998), during which time anomalously  
242 warm waters encroached eastwards into the Great Australian Bight from western Australia  
243 (see also Savin et al., 1975; Gourley and Gallagher, 2004).

244 Our study shows that seismic reflection data can image erosional and depositional  
245 features that provide a physical stratigraphic record of ancient ocean currents. We  
246 demonstrate that by placing these features into a broad chronostratigraphic framework, we  
247 can complement rather sparse micro-faunal evidence, and gain important insights into the  
248 timing of onset of major ocean currents. Data limitations notwithstanding, our seismic  
249 reflection-based approach does, at the very least, provide a clear hypothesis testable with  
250 future scientific drilling (e.g. IODP). Seismic reflection data allow erection of a physical,  
251 stratigraphic framework and remains an essential part of the paleoceanographer's toolkit.  
252 Future work should focus on detailed mapping of seismic reflection datasets from, for  
253 example, the western Bight Basin and Otway Basin; this may reveal similar, age-equivalent  
254 current-formed stratigraphic features, thus raising the possibility that the proto-Leeuwin  
255 Current extended further eastwards and influenced faunal distribution and potentially climate  
256 over a wider area than currently assumed.

257

## 258 **ACKNOWLEDGEMENTS**

259 Geoscience Australia are thanked for providing seismic and borehole data. We are especially  
260 thankful to journal reviewers Sam Johnstone and Brian Romans for providing such insightful,  
261 constructive reviews of our paper, and to Andrea Fildani and Gary Hampson for their  
262 editorial handling.

263

## 264 **REFERENCES**

265

266 Boldreel, L.O.L., Andersen, M.S., and Kuijpers, A., 1998, Neogene seismic facies and deep-  
267 water gateways in the Faeroe Bank area, NE Atlantic: *Marine Geology*, v. 152, p. 129-140.

268

269 Boyle, P.R., Romans, B.W., Tucholke, B.E., Norris, R.D., Swift, S.A., and Sexton, P.F.,  
270 2017, Cenozoic North Atlantic deep circulation history recorded in contourite drifts, offshore  
271 Newfoundland, Canada: *Marine Geology*, v. 385, p. 185-203.

272

273 Callaway, A., Smyth, J., Brown, C.J., Quinn, R., Service, M., and Long, D., 2009, The  
274 impact of scour processes on a smothered reef system in the Irish Sea: *Estuarine, Coastal and*  
275 *Shelf Science*, v. 84, p. 409–418.

276

277 Campbell, D.C., Mosher, D.C., 2015. Geophysical evidence for widespread Cenozoic bottom  
278 current activity from the continental margin of Nova Scotia, Canada: *Marine Geology*, v.  
279 378, p. 237-260.

280

281 Caputi, N., Chubb, C.F., and Pearce, A., 2001, Environmental effects on recruitment of the  
282 western rock lobster, *Panulirus Cygnus*: *Marine and Freshwater Research*, v. 52, p. 1167-  
283 1175.

284

285 Cann, J.H., and Clarke, J.A.D., 1993, The significance of *Marginopora vertebralis*  
286 Foraminifera in surficial sediments at Esperance, Western Australia and in last interglacial  
287 sediments in northern Spencer Gulf: *Marine Geology*, v. 111, p. 171–187.

288

289 Cresswell, G., and Goldring, T., 1980, Observations of a south-flowing current in the  
290 southeastern Indian Ocean: *Deep Sea Research Part 1: Oceanographic Research Papers*, v.  
291 27, p. 449-466.

292

293 Cresswell, G.R., and Domingues, C.M., 2009, The Leeuwin Current south of Western  
294 Australia: *Journal of the Royal Society of Western Australia*, 92: 83–100, 2009

295

296 Davies, R.J., Cartwright, J.A., Pike, J., and Line, C., 2001, Early Oligocene initiation of  
297 North Atlantic deep water formation: *Nature*, v. 410, p. 917-920.

298

299 Due, L., van Aken, H.M., Boldreel, L.O., and Kuijpers, A., 2006, Seismic and oceanographic  
300 evidence of present-day bottom-water dynamics in the Lousy Bank-Hatton Bank area, NE  
301 Atlantic. *Deep Sea Research Part 1: Oceanographic Research Papers*, v. 53, p. 1729-1741.

302

303 Espurt, N., Callot, J-P., Totterdell, J., Struckmeyer, H., and Vially, R., 2009, Interaction  
304 between continental breakup dynamics and large-scale delta system evolution: insights from  
305 the Cretaceous Ceduna delta system, Bight Basin, southern Australian margin: *Tectonics*, v.  
306 28, TC6002.

307

308 Faugères, J.C., Stow, D.A.V, Imbert, P., and Viana, A., 1999, Seismic features diagnostic of  
309 contourite drifts. *Marine Geology*, v. 162, p. 1-38.

310

311 Feary, D.A., and James, N.P., 1995, Cenozoic biogenic mounds and buried Miocene (?)  
312 barrier reef on a predominantly cool-water carbonate continental margin, Eucla Basin,  
313 western Great Australian Bight: *Geology*, v. 23, p. 427-430.

314

315 Feary, D.A., and James, N.P., 1998, Seismic Stratigraphy and Geological Evolution of the  
316 Cenozoic, Cool-Water Eucla Platform, Great Australian Bight: *AAPG Bulletin*, v. 82, p. 792-  
317 816.

318

319 Feng, M., Waite, A., and Thompson, P., 2009, Climate variability and ocean production in  
320 the Leeuwin Current system off the west coast of Western Australia: *Journal of the Royal*  
321 *Society of Western Australia*, v. 92, p. 67-81.

322

323 Gourley, T.L., and Gallagher, S.J., 2004, Foraminiferal biofacies of the Miocene warm to  
324 cool climatic transition in the Port Phillip Basin, southeastern Australia: *Journal of*  
325 *Foraminiferal Research*, v. 34, p. 294-307.

326

327 Henderson, G.M., 2002, New oceanic proxies for paleoclimate, *Earth and Planetary Science*  
328 *Letters*, v. 203, 1-13.

329

330 Hohbein, M., Sexton, P.F., and Cartwright, J.A., 2012, Onset of North Atlantic Deep Water  
331 production coincident with inception of the Cenozoic global cooling trend: *Geology*, v. 40, p.  
332 255-258.

333

334 Huber, M., Brinkhuis, H., Stickley, C.E., Döös, K., Sluijs, A., Warnaar, J., Schellenberg,  
335 S.A., and Williams, G.L., 2004, Eocene circulation of the Southern Ocean: Was Antarctica  
336 kept warm by subtropical waters? *Paleoceanography*, v. 19, PA4026.

337

338 IPCC, 2007, *Climate Change 2007: The physical science basis. Contribution of Working*  
339 *Group I to the Fourth Assessment Report of the Intergovernmental Panel on Climate Change*

340 (eds. Solomon, S., Qin, D., Manning, M., Chen, Z., Marquis, M., Averyt, K.B., Tignor, M.,  
341 and Miller, H.L.). Cambridge University Press, Cambridge.  
342

343 Jackson, C.A-L., 2012, Seismic reflection imaging and controls on the preservation of ancient  
344 sill-fed magmatic vents: *Journal of the Geological Society*, v. 169, p. 503-506.  
345

346 Janocko, M., Nemeč, W., Henriksen, S. and Warchoł, M., 2013, The diversity of deep-water  
347 sinuous channel belts and slope valley-fill complexes. *Marine and Petroleum Geology*, 41,  
348 p.7-34.  
349

350 MacLachlan, S.E., Elliott, G.M., and Parsons, L.M., 2008, Investigations of the bottom  
351 current sculpted margin of the Hatton Bank, NE Atlantic: *Marine Geology*, v. 253, p. 170-  
352 184.  
353

354 Magee, C., Hunt-Stewart, E., and Jackson, C.A-L., 2013, Volcano growth mechanisms and  
355 the role of sub-volcanic intrusions: Insights from 2D seismic reflection data: *Earth and*  
356 *Planetary Science Letters*, 373, p. 41-53.  
357

358 McGowran, B., Qianyu, L., Cann, J., Padley, D., McKirdy, D.M., and Shafik, S., 1997,  
359 Biogeographic impact of the Leeuwin Current in southern Australia since the late Middle  
360 Eocene: *Palaeogeography, Palaeoclimatology, Palaeoecology*, v. 136, p. 19-40.  
361

362 Müller-Michaelis, A., Uenzelmann-Neben, G., and Stein, R., 2013, A revised Early Miocene  
363 age for the instigation of the Eirik Drift, offshore southern Greenland: Evidence from high-  
364 resolution seismic reflection data: *Marine Geology*, v. 340, p. 1-15.  
365

366 Posamentier, H.W. and Kolla, V., 2003, Seismic geomorphology and stratigraphy of  
367 depositional elements in deep-water settings. *Journal of sedimentary research*, 73, p. 367-388.  
368

369 O'Reilly, B., Readman, P.W., Shannon, P.M., and Jacob, A.W.B., 2003, A model for the  
370 development of a carbonate mound population in the Rockall Trough based on deep-towed  
371 sidescan sonar data: *Marine Geology*, v. 198, p. 55-66.  
372

373 Rahmstorf, S., 2003, The current climate: *Nature*, v. 421, p. 699.

374

375 Rebesco, M., and Stow, D., 2001, Seismic expression of contourites and related deposits: a  
376 preface: *Marine Geophysical Researches*, v. 22, p. 303–308.

377

378 Rebesco, M., Hernández-Molina, F.J., Van Rooij, D., Wåhlin, A., 2014. Contourites and  
379 associated sediments controlled by deep-water circulation processes: state-of-the-art and  
380 future considerations: *Marine Geology*, 352, p.111-154.

381

382 Rollet, N., McGiveron, S., Hashimoto, T., Hackney, R., Petkovic, P., Higgins, K., Grosjean,  
383 E., Logan, G.A., 2012, Seafloor features and fluid migration in the Capel and Faust basins,  
384 offshore eastern Australia: *Marine and Petroleum Geology*, v. 35, p. 269–291.

385

386 Savin, S.M., Douglas, R.G., and Stehli, F.G., 1975, Tertiary marine paleotemperatures:  
387 *Geological Society of American Bulletin*, v. 86, p. 1499–1510.

388

389 Schofield, A., and Totterdell, J., 2008, Distribution, timing and origin of magmatism in the  
390 Bight and Eucla basins: Australian Government Report, 2008/24.

391

392 Shafik, S., 1983, Calcareous nannofossil biostratigraphy: an assessment of foraminiferal and  
393 sedimentation events in the Eocene of the Otway Basin, southeastern Australia: *Journal of*  
394 *Australian Geology and Geophysics*, v. 8, p. 1-17.

395

396 Shafik, S., 1990, The Maastrichtian and early Tertiary record of the Great Australian Bight  
397 Basin and its onshore equivalents on the Australian southern margin: a nannofossil study:  
398 Bureau of Mineral Resources *Journal of Australian Geology and Geophysics*, v. 11, p. 473-  
399 497.

400

401 Stickley, C.E., Brinhuis, H., Schellenberg, S.A., Sluijs, A., Röhl, U., Fuller, M., Grauert, M.,  
402 Huber, M., Warnaar, J., and Williams, G.L., 2004, Timing and deepening of the Tasmanian  
403 Gateway. *Paleoceanography*, v. 19: PA4027.

404

405 Stow, D.A.V., Faugères, J.C., Howe, J.A., Pudsey, C.J., and Viana, A.R., 2003, Bottom  
406 currents, contourites and deep-sea sediment drifts: Current state-of-the-art, in Stow, D.A.V.,

407 et al., eds., Deep-water contourite systems: Modern drifts and ancient series, seismic and  
408 sedimentary characteristics: The Geological Society of London Memoir, v. 22, p. 73–84.

409

410 Tucholke, B.E., 1979, Relationships between acoustic stratigraphy and lithostratigraphy in  
411 the western North Atlantic Basin, in: Tucholke, B.E., Vogt, P.R. (Eds.), Initial Reports of the  
412 Deep Sea Drilling Project, Vol. 43. U.S. Government Printing Office, Washington, D.C., pp.  
413 827-846.

414

415 Tucholke, B.E., and Mountain, G.S., 1979, Seismic stratigraphy, lithostratigraphy and  
416 paleosedimentation patterns in the North American Basin, in: Talwani, M., Hay, W., Ryan,  
417 W.B.F. (Eds.), Deep Drilling in the Atlantic Ocean: Continental Margins and  
418 Paleoenvironment, Maurice Ewing Series 3. American Geophysical Union, Washington,  
419 D.C., pp. 58-86.

420

421 von Blanckenburg, F., 1999, Palaeoceanography: tracing past ocean circulation?: Science, v.  
422 286, p. 1862-1863.

423

424 Wunsch, C., 2002, What is the thermohaline circulation?: Nature, v. 298, p. 1179-1181.

425

426 Wyrwoll, K-H., Greenstein, B.J., Kendrick, G.W., and Chen, G.S., 2009, The  
427 palaeoceanography of the Leeuwin Current: implications for a future world. Journal of the  
428 Royal Society of Western Australia, v. 92, p. 37–51.

429

### 430 **FIGURE CAPTIONS**

431

432 **Fig 1.** (A) Map illustrating the geographical setting of the study area. The area covered by 2D  
433 seismic reflection data is outlined by a solid black line. Inset shows the key modern  
434 oceanographic currents developed along the western and southern Australian margin.  
435 LC=Leeuwin Current; ACC=Antarctic Circumpolar Current; WAC=West Australia Current;  
436 FC=Flinders Current. OB=Otway Basin. Modified from Jackson (2012); oceanographic  
437 currents from Bilj et al. (2013). Grey dashed lines indicate boundaries between sub-basins  
438 forming part of the Great Australian Bight. (B) Simplified stratigraphic column based on data  
439 from boreholes Gnarlyknots-1A and Potoroo-1. Key seismic horizons (A–D) and seismic  
440 units (SU1-2) are indicated. The stratigraphic occurrence of intrusion and extrusive

441 components of the Bight Basin Igneous Complex (BBIC) are shown. Modified from Jackson  
442 (2012).

443

444 **Fig. 2.** Time-structure map of the Horizon B (base Nullarbor Limestone) clipped where it  
445 intersects Horizon C (top volcanic vents); this illustrates the distribution of volcano summits  
446 (labelled 'v' and encircled by a solid white line) that rise above Horizon D, and intra-SU2  
447 scours (labelled 's'). d=drifts. (A) and (B) are from the southern and northern parts of the  
448 study area respectively. See Figure 1A for location of map. Light grey lines indicate seismic  
449 reflection profiles. Note that the geometries of the Horizons C and D are poorly constrained  
450 away from the 2D seismic reflection profiles.

451

452 **Fig. 3.** (A)–(D) Interpreted seismic profiles illustrating the geometry, scale and relationship  
453 between extrusive volcanic features of the Bight Basin Igneous Complexes and intra-  
454 Nullarbor Limestone contourites (i.e. scours and bedforms). Locations of the seismic lines are  
455 shown in Figure 2. Note the vertical scale is provided in ms TWT and metres, based on an  
456 intra-Nullarbor interval velocity of  $2100 \text{ m s}^{-1}$ . Uninterpreted versions of sections are  
457 available in DR11.

458

459 **Fig. 4.** (A–C) Schematic diagrams illustrating the evolution of intra-Nullarbor Limestone  
460 contourites in the Great Australia Bight. The vertical dashed line in the 'current strength'  
461 column indicates the threshold for sediment erosion/non-deposition; these conditions occur at  
462 the onset of T2.

463

464 **Data Repository Item (DR1).** Uninterpreted versions of the seismic profiles presented in  
465 Fig. 3.

Fig. 1

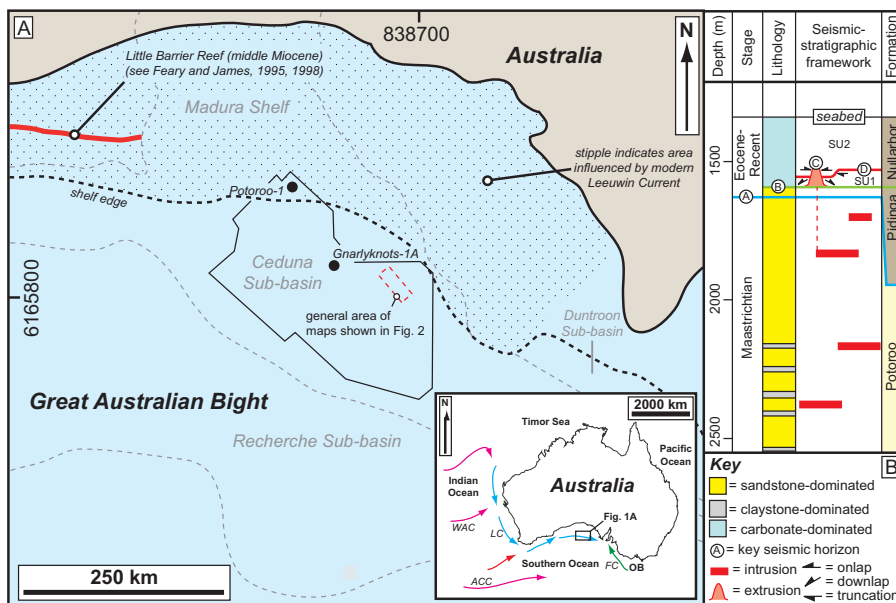




Fig. 2

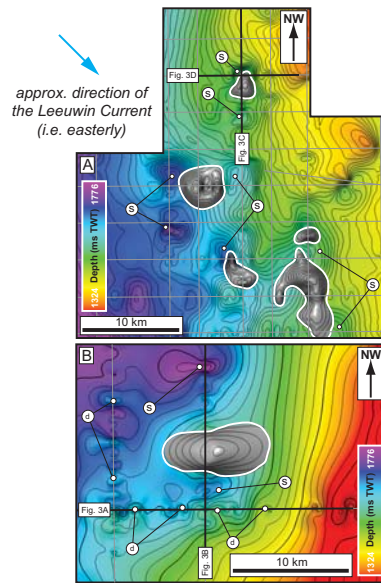


Fig. 3

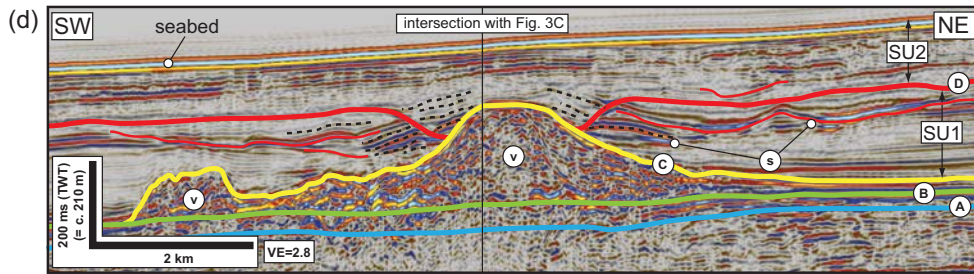
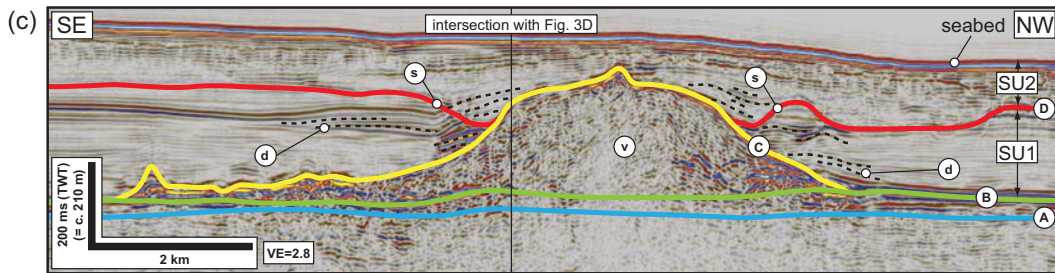
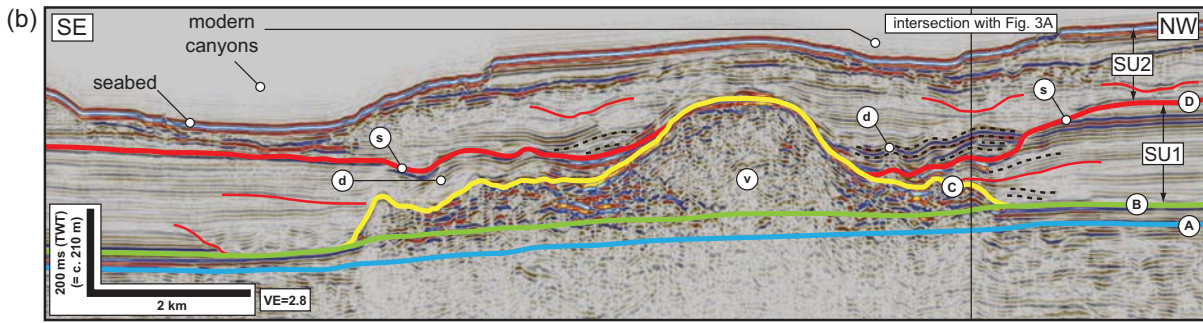
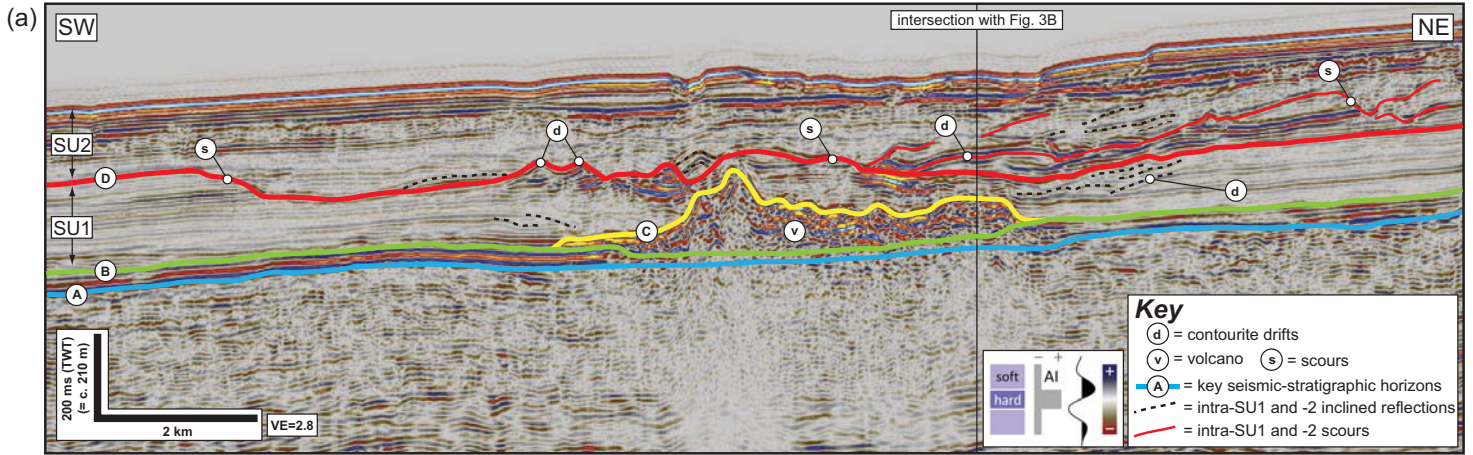


Fig. 4

